Differential Cysteine Labeling and Global Label-Free Proteomics Reveals an Altered Metabolic State in Skeletal Muscle Aging

Brian McDonagh,*,[†] Giorgos K. Sakellariou,[†] Neil T. Smith,[†] Philip Brownridge,[‡] and Malcolm J. Jackson[†]

[†]MRC-Arthritis Research UK Centre for Integrated Research into Musculoskeletal Aging (CIMA), Skeletal Muscle Pathophysiology Research Group, Institute of Ageing and Chronic Disease, [‡]Protein Function Group, Institute of Integrative Biology, University of Liverpool, Liverpool L69 3GA, United Kingdom

S Supporting Information

ABSTRACT: The molecular mechanisms underlying skeletal muscle aging and associated sarcopenia have been linked to an altered oxidative status of redox-sensitive proteins. Reactive oxygen and reactive nitrogen species (ROS/RNS) generated by contracting skeletal muscle are necessary for optimal protein function, signaling, and adaptation. To investigate the redox proteome of aging gastrocnemius muscles from adult and old male mice, we developed a label-free quantitative proteomic approach that includes a differential cysteine labeling step. The approach allows simultaneous identification of up- and downregulated proteins between samples in addition to the identification and relative quantification of the reversible oxidation state of susceptible redox cysteine residues. Results from muscles of adult and old mice indicate significant changes in the content of chaperone, glucose metabolism, and cytoskeletal regulatory proteins, including Protein DJ-1, cAMP-dependent protein kinase type II, 78 kDa glucose regulated protein, and a reduction in the number of redox-responsive proteins identified in muscle of old mice. Results demonstrate skeletal muscle aging causes a reduction in redox-sensitive proteins involved in the generation of precursor metabolites and energy metabolism, indicating a loss in the flexibility of the redox energy response. Data is available via ProteomeXchange with identifier PXD001054.

KEYWORDS: *Redox proteomics, aging, skeletal muscle metabolism, Grp78, aconitase and sirtuin1*
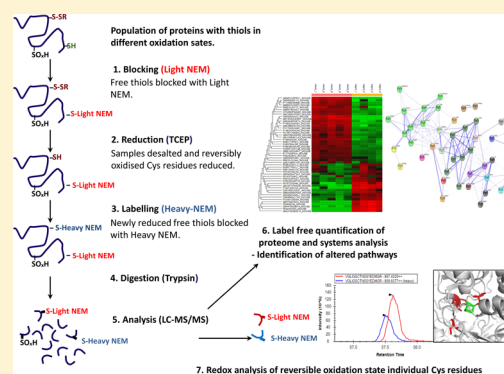
INTRODUCTION

Skeletal muscle represents a unique and physiologically relevant model for the analysis of redox signaling during aging. Contracting skeletal muscle generates reactive oxygen and reactive nitrogen species (ROS/RNS) necessary for correct protein function, signaling, and adaptation.[1−3] Many key processes within the cell and essential regulatory proteins involved in excitation−contraction coupling require reversible redox modifications of specific cysteine (Cys) residues for their activation (or inactivation), cofactor and substrate binding, e.g., sarcoplasmic/endoplasmic reticulum Ca^{2+} ATPase (SERCA) and ryanodine receptor 1 (Ryr1).[4,5] ROS/RNS generated within skeletal muscle fibers can originate from both mitochondrial and non-mitochondrial sources.[6] Electron leakage from the mitochondrial electron transport chain accounts for a portion of the ROS produced, but it is increasingly recognized that the NAD(P)H oxidase (NOX) and nitric oxide synthase (NOS) families, due to their abundance and subcellular location in muscle fibers, play a crucial role in skeletal muscle ROS/RNS generation.[6] A number of factors may influence the concentration and species of ROS/RNS generated as a result of muscle contractions including muscle fiber type, the intensity of the exercise, and the age and fitness of the individual.

Aging muscle has an altered redox response with subsequent physiological and biochemical effects on the cytoskeleton, mitochondria, calcium signaling, and sequestration.[7−9] The species and concentrations of ROS/RNS generated as a result of contractions will have a major influence on the adaptive and therapeutic responses sought through exercise, with wide long-term effects on a host of biochemical processes within the cell. The activity of regulatory proteins situated at the cross roads of key metabolic processes are known to be modified by ROS/ RNS influencing their activity and metabolic flux within the cell or muscle fibers.[10] ROS/RNS are, in general, too reactive to have a signaling effect as a result of diffusion throughout the cell, and their reactivity suggests they will have an effect localized to their site of generation.[11] Redox-sensitive proteins including cytoskeletal proteins are attractive candidates for the propagation of the redox signal, potentially initiating a cascade of reactions on sensitive residues within those proteins.[12] It has also been demonstrated that proteins with surface thiols
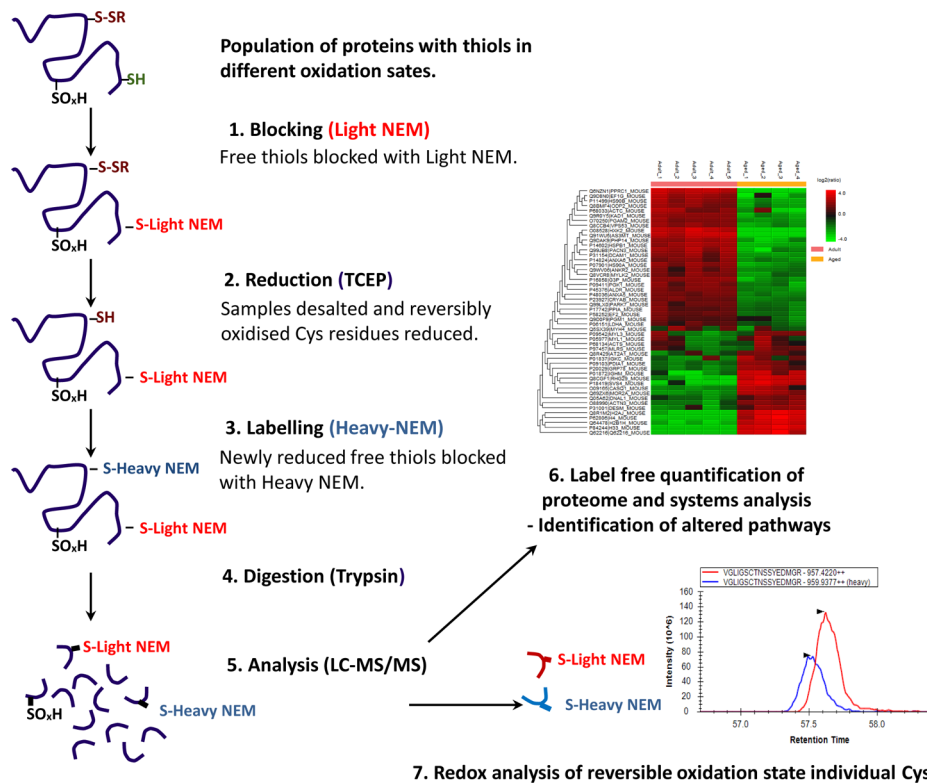
Figure 1. Schematic illustration of the approach used to analyze the redox proteome. (1) Samples are lysed in a buffer containing the alkylating reagent d(0) NEM. (2) Excess NEM is removed by desalting, and reversibly oxidized Cys residues are reduced using TCEP. (3) Newly reduced Cys residues are alkylated with the heavy isotopic form of NEM (d5-NEM). (4) Samples are digested using trypsin. (5) Peptides analyzed by LC−MS/MS using QExactive. (6) Label-free quantification of proteins is performed using PEAKS software. (7) Reversible oxidation state of individual Cys redox peptides are relatively quantified using the targeted quantification program Skyline.

represent the dominant intra-mitochondrial thiols and may function as a redox buffer.[13]

Reversible thiol disulfide exchange on specific Cys residues within proteins offers a rapid and flexible means to modify target proteins by altering both the structure and activity of the proteins.[14] The major reversible Cys oxidative modifications include sulfenic acid (-SOH), disulfide bond formation (-S-S-), glutathionylation (-SSG), and nitrosylation (-SNO) as well as the largely irreversible modifications sulfinic (-SO$_2$H) and sulfonic (-SO$_3$H) acid formation. Irreversible oxidative modifications as a result of excessive ROS/RNS can lead to insoluble protein aggregates and protein degradation, which have been reported to increase in aging and neurodegenerative diseases.[15] Identification of proteins that are reversibly modified and relative quantification of the redox state of the susceptible Cys residues within those proteins would help in our understanding of the redox processes and pathways involved in biological aging.

In the present study, we have applied a novel redox proteomic approach to gastrocnemius muscles of adult and old mice to identify and quantify the reversible redox state of specific Cys residues within individual muscle samples and to quantify relative protein abundance between samples. The redox approach includes a differential Cys labeling step by taking advantage of a chemically equivalent heavy (d5) and light (d0) isotopic form of the common thiol alkylating reagent N-ethylmaleimide (NEM). Differential labeling of reversibly oxidized and reduced Cys residues utilizing a heavy isotopic form of the same alkylating compound keeps the labeling chemistry constant, and the chemical moiety behaves identically

in the mass spectrometer. Targeted analysis of the differentially labeled Cys residues within a sample was performed using the open source proteomic software Skyline,[16] whereas label-free quantification was performed with PEAKS 7 software for relative protein quantification between samples.[17] Combining the quantification of the reversible oxidation state of specific Cys residues and a complementary label-free relative quantification is an essential component of the technique, as many redox-sensitive proteins may not change in abundance but their activity can be altered significantly by alterations in the redox state of susceptible Cys residues, providing additional information on the functional proteome. We have applied this technique to gastrocnemius muscles from adult and old mice, which are known to undergo atrophy with age.[18] We also complimented the high-throughput proteomics approach with analysis of common indicators of oxidative stress, western blotting of the content of individual proteins, and, where possible, enzyme activity assays. Results indicate that there are significant differences in both the proteome and the oxidative state of redox-sensitive proteins from skeletal muscle of adult and old mice.

■ EXPERIMENTAL METHODS

Materials and Reagents

All reagents and chemicals including heavy (d5) and light (d0) isotopic forms of NEM were obtained from Sigma-Aldrich (Dorset, UK) unless otherwise stated and were of analytical grade or above.

Animals

Adult (12 months) and old (25 months) C57BL/6 male mice were purchased from Charles River and housed in the Specific Pathogen-Free (SPF) Facility at the University of Liverpool for at least 2 weeks before use. Experiments were performed in accordance with U.K. Home Office Guidelines under the U.K. Animals (Scientific Procedures) Act 1986 and received ethical approval from the University of Liverpool Animal Welfare and Ethical Review Board. Animals were sacrificed by cervical dislocation, and gastrocnemius muscles were immediately dissected. A gastrocnemius muscle from each mouse was placed immediately in thiol blocking buffer containing 25 mM d(0) NEM and 50 mM ammonium bicarbonate, pH 8, for redox proteomic analysis. The corresponding gastrocnemius muscle from each mouse was snap-frozen in liquid nitrogen and stored at −80 °C until processed.

Protein Extraction for Redox Proteomics

A schematic of the redox approach is outlined in Figure 1. Briefly, protein extracts for redox analysis from adult ($n = 5$) and old ($n = 4$) mice were prepared using a hand homogenizer in the presence of thiol blocking buffer containing d(0) NEM under anaerobic conditions. Protein lysates were cleared by centrifugation at 15 000g for 10 min at 4 °C, and protein concentrations were calculated by Bradford assay (BioRad, Hertfordshire, UK) using BSA as a standard. Protein extracts for redox analysis were desalted using Zeba spin desalting columns (Thermo Scientific, Hemel, Hempstead, UK), and protein concentrations were recalculated as before. Two hundred micrograms of the desalted protein extract was diluted up to 160 μL with 25 mM ammonium bicarbonate and denatured by addition of 10 μL of 1% w/v RapiGest (Waters, Manchester, UK) in 25 mM ammonium bicarbonate and followed by incubation at 80 °C for 10 min. Reversibly oxidized Cys residues were reduced by the addition of 10 μL of 100 mM TCEP and incubated at 60 °C for 10 min. Cys residues that were reduced at this stage were subsequently alkylated with 10 μL of 200 mM d(5) NEM and incubated at room temperature for 30 min. Trypsin (Sigma, Poole, UK) was reconstituted in 50 mM acetic acid, and 2 μg was added to the samples followed by incubation overnight at 37 °C. The digestion was terminated and RapiGest removed by acidification (3 μL of TFA and incubation at 37 °C for 45 min) and centrifugation (15 000g for 15 min).

LC−MS/MS and Label-Free MS Quantification

The data-dependent label-free analysis was performed using an Ultimate 3000 RSLC nano system (Thermo Scientific) coupled to a QExactive mass spectrometer (Thermo Scientific). The sample (5 μL corresponding to 250 ng of protein) was loaded onto the trapping column (Thermo Scientific, PepMap100, C18, 75 μm × 20 mm), using partial loop injection, for 7 min at a flow rate of 4 μL/min with 0.1% (v/v) TFA. The sample was resolved on the analytical column (Easy-Spray C18 75 μm × 500 mm, 2 μm column) using a gradient of 97% A (0.1% formic acid) and 3% B (99.9% ACN and 0.1% formic acid) to 60% A and 40% B over 120 min at a flow rate of 300 nL/min. The data-dependent program used for data acquisition consisted of a 70 000 resolution full-scan MS scan (AGC set to 10^6 ions with a maximum fill time of 250 ms), and the 10 most abundant peaks were selected for MS/MS using a 17 000 resolution scan (AGC set to 5 × 10^4 ions with a maximum fill time of 250 ms) with an ion selection window of 3 m/z and a normalized collision energy of 30. To avoid repeated selection of peptides for MS/MS, the program used a 30 s dynamic exclusion window.

Raw spectra were converted to mascot generated files (mgf) using Proteome Discoverer software (Thermo Scientific). The resulting mgf files were searched against the UniProt mouse sequence database (12/05/2012, 16 376 sequences) using an in-house Mascot server (Matrix Science, London, UK). Search parameters used were as follows: peptide mass tolerances, 10 ppm; fragment mass tolerance, 0.01 Da, 1+, 2+, and 3+ ions; missed cleavages, 1; instrument type, ESI-TRAP. Variable modifications included were as follows: d(0) NEM, d(5) NEM, mono-, di-, and trioxidation of cysteine residues and oxidation of methionine. Label-free relative quantification software PEAKS 7 (Bioinformatics Solutions Inc., Waterloo, Canada) was used to analyze RAW data files against the same mouse protein database for identifications with Mascot.[17] Proteins were considered significantly changed between adult and old mouse protein samples using a −10 log P score of 20 (equivalent to a p value of 0.01), a fold change ≥ 1.5, and using a quality value of 0.8. Statistical analysis of protein and peptide features and the full list of the significantly changed proteins, the peptides used for identification across all samples, and analysis of MS data are included in Supporting Information files 1 and 2. PEAKS 7 software includes a post-translational modification (PTM) algorithm applying the de novo sequencing module within the software to search for a limited number of PTMs. All peptides identified during de novo sequencing are evaluated under the same −log P score and FDR validation. Supporting Information file 3 contains the list of K-acetylated proteins identified from adult and old mice with the fragmentation of K-acetylated peptide common to histone H.3.2. The mass spectrometry proteomics data has been deposited with the ProteomeXchange Consortium (http://proteomecentral.proteomexchange.org) via the PRIDE partner repository[19] with the data set identifier PXD001054. All proteomic data has been uploaded and is publically available through the ProteomeXchange consortium

Targeted Analysis of Differentially Labeled Cys Residues

Cys-containing peptides detected with identical amino acid sequences and both d(0) and d(5) NEM modifications independently with an individual peptide ion Mascot score of >20 were considered redox peptides. Redox peptides detected from Proteome Discovery analyses of RAW files were selected for targeted analysis using m/z data and retention times with the open software Skyline.[16] Targeted analysis applying m/z, retention times, and fragmentation spectra for peptide selection allowed the calculation of the reduced/oxidized ratio (or d(0)/d(5) NEM) of the Cys residues using the individual parent ion intensities with Skyline. The individual reduced/oxidized ratio for redox Cys peptides in each sample was used to calculate an average ratio of reduced/oxidized calculated for the specific Cys residues. Intensities of targeted peptides are included in Supporting Information file 4.

Immunoblotting and Aconitase Activity

Homogenates of muscle from adult ($n = 5$) and old ($n = 5$) mice were prepared using RIPA buffer containing 50 mM Tris (pH 7.4), 150 mM NaCl, and protease inhibitors. Equal amounts of protein (20−50 μg, depending on the protein of interest) were separated by SDS-PAGE and transferred onto nitrocellulose membranes. All membranes were stained with Ponceau S (0.2% w/v) in 5% acetic acid (v/v) to ensure equivalent protein loading and transfer. Preliminary data
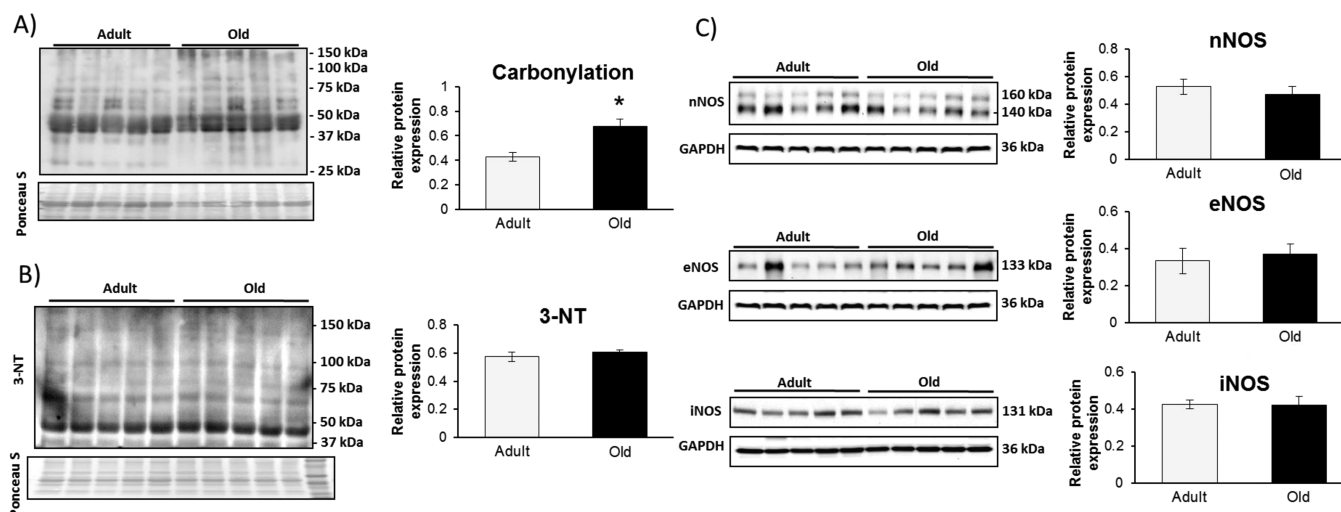
Figure 2. Indicators of oxidative stress in gastrocnemius muscles from adult and old mice show an increase in protein carbonylation (A) and no change in 3-nitrotyrosine (3-NT) content (B). The muscle content of the three nitric oxide synthase isoforms (C) showed no change between adult and old mice.

showed that Ponceau S staining corresponded to GAPDH protein expression (data not shown in detail); hence, relative protein abundance was analyzed densitometrically and standardized using GAPDH or Ponceau S staining. Membranes were probed using the following primary antibodies: anti-Sirt1, anti-crystallin, anti-grp78, anti-GST P1, anti-GST mu, anti-Trx, anti-Txnip, anti-Acon2, anti-NOS1−3, anti-Prdx3−6, anti-acetyl K, anti-GAPDH, anti-Trx, anti-Srxn, anti-Gpx1 and anti-catalase from Abcam (Cambridge, UK); anti-3NT, anti-SOD1−3, and anti-Hsp70 were from Stressgen (Exeter, UK), and anti-DNP was from Invitrogen (Thermo Scientific). Protein carbonylation was performed as previously described.[20] HRP-conjugated anti-mouse and anti-rabbit antibodies were purchased from Cell Signaling Technologies (Hitchin, UK). Bands were detected using an ECL kit (Amersham International, Cardiff, UK), and band intensities were analyzed using ImageJ software 1.45b (NIH, USA). Single comparisons between the experimental age groups were performed using Student's unpaired t test, and data are presented as mean ± SEM. Data were analyzed using SPSS 18, and p-values <0.05 were considered to be statistically significant.

Aconitase enzyme activity was analyzed as previously described.[21] Briefly, activity was measured using the reduction of $NADP^+$ to NADPH by fluorescence, excitation 360 nm and emission 460 nm, over 15 min. The reaction mixture contained 50 mM Tris HCl, pH 7.5, 5 mM sodium citrate, 0.6 mM $MnCl_2$, 0.2 mM $NADP^+$, 2 units of isocitrate dehydrogenase/mL, and 50−100 μg of protein/mL. Aconitase activity is expressed as units of NADPH produced/min/mg of protein.

■ RESULTS

Oxidative Stress Indicators in Skeletal Muscle from Adult and Old Mice

Protein extracts from gastrocnemius muscles of adult and old mice were analyzed for global indicators of oxidative stress: irreversible protein modifications including carbonylation and 3-nitrotyrosine (3-NT) formation. There was a significant increase in carbonylated proteins revealed by immunoblotting, but no increase in overall 3-NT content was detected (Figure 2, panels A and B, respectively). No increase was observed in the

expression levels of the three nitric oxide synthase (NOS) isoforms (neuronal NOS, inducible NOS, and endothelial NOS) (Figure 2C).

Label-Free Proteomic Analysis of Skeletal Muscle from Adult and Old Mice

Over 500 unique proteins were confidently identified in each sample using shotgun proteomics and Proteome Discoverer software. Label-free quantification was performed using PEAKS 7 software to determine proteins that were differentially regulated between protein samples from adult and old mice with a p value < 0.01 and a minimum fold change of 1.5 between groups. Overall, 47 proteins were detected as significantly altered: 32 proteins were downregulated and 15 proteins were upregulated with age (Figure 3A). Proteins that showed significant differences were analyzed by the database for annotation, visualization, and integrated discovery (DAVID)[22] and String-DB for known and predicted protein−protein interactions.[23] DAVID analysis and functional annotation clustering of upregulated proteins in the samples from adult mice indicated that glucose metabolism was upregulated in adult mice compared with that in old mice (enrichment score 7.54, p value 1.2×10^{-11}). Similar enrichment and metabolic processes were identified from String-DB (Figure 3C). A number of regulatory chaperone and heat shock proteins whose expression is related to metabolic state were found to be relatively decreased in the samples from old mice, including protein DJ-1 (Park7), αB cyrstallin (Cryab), adenylate kinase (Ak1), cAMP regulatory kinase (AMPK) α (Prkara2), glutathione S-transferase P1 (Gst P1), heat shock protein beta-1 (Hspb1), and heat shock protein 90-alpha (Hsp90aa1) and -beta (Hsp90ab1). Label-free quantification indicated an upregulation of core components of the nucleosome in muscles from old mice: histones H2A, H2B, H3.3, and H4 (Figure 3A). Functional annotation clustering of upregulated proteins in the samples from old mice (Figure 3C) indicated an enrichment of methylation and histone core proteins (enrichment score 4.54, p value 2.7×10^{-8}).

In order to validate the label-free quantification approach, immunoblotting of a number of the differentially regulated proteins was performed. Figure 3B shows immunoblots and densitometry of the bands for Grp78, Gst P1, Hsp70, and
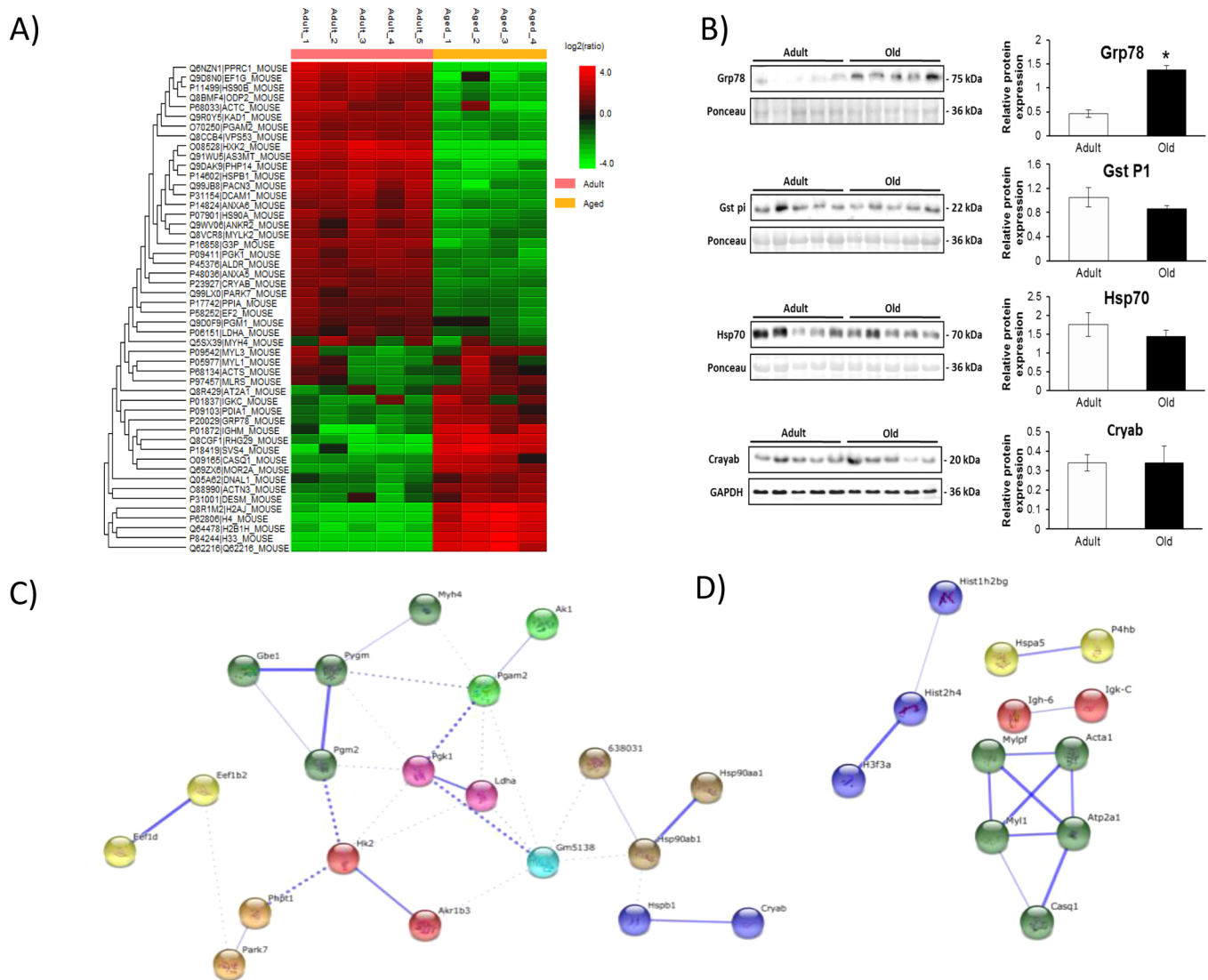
Figure 3. (A) Heatmap of significantly up- and downregulated proteins in gastrocnemius mouse tissue from adult and old mice detected by PEAKS label-free quantification software ($p < 0.01$, min fold change >1.5, quality 0.8, and at least one unique peptide). (B) Western blotting for Grp78, Gst P1, Hsp70, and Cryab. (C) String-DB analysis of up- and downregulated proteins in samples from adult vs old mice. Upregulated proteins in samples from adult mice are enriched for carbohydrate catabolic processes as analyzed by String-DB analysis ($p = 2.12 \times 10^{-6}$). (D) Upregulated proteins in samples from old mice are enriched for skeletal muscle contraction proteins ($p = 8.44 \times 10^{-2}$). Stronger associations are represented by thicker lines.

Cryab. Grp78 is an endoplasmic reticulum protein and an indicator of ER stress response.[24] Immunoblotting confirmed the label-free quantification result, with a significant increase in samples from old mice. Gst P1 has been associated with detoxification of proteins and as a reductant of the 1-Cys peroxiredoxin 6.[25] Immunoblotting for Gst P1 suggested a slight increase in adult mice, but quantification of the bands indicated that the groups were not significantly different. The small heat shock protein Cryab has chaperone-like activity and has been associated with the prevention of aggregation of a number of proteins involved in the stress response.[26] Immunoblotting indicated no difference between samples from adult and old mice, but the label-free quantification showed a decreased content with age. The discrepancy between data obtained with label-free analysis and immunoblotting may be due to a number of reasons, including the use of different muscles (the contralateral muscle was used for immunoblotting), the specificity of the primary antibody, protein abundance, and the method of label-free quantification.

Acetylated Proteins in Skeletal Muscle from Adult and Old Mice

There was an increase in core nucleosome proteins known to be regulated by acetylation in protein samples from old mice: histones H2A, H2B, H3.3, and H4. This prompted us to investigate overall acetylation levels on Lys residues within the samples. A number of specific proteins showed increased acetylation levels with aging, suggesting an altered response (Figure 4A). Searching the PEAKS PTM finder, a number of proteins were identified as containing Lys-acetylated modification. There were specific proteins that were acetylated only in samples from old mice. Supporting Information file 3 contains a list of the proteins identified and the fragmentation spectra of Lys-acetylated peptide from histone H2.

The samples were also probed against the class III NAD$^+$-dependent deacetylase Sirt1, one of the major regulators of the oxidative stress response that is regulated by its redox state.[27] There was a significant increase in Sirt1 protein levels in samples from old mice compared to that from adult mice
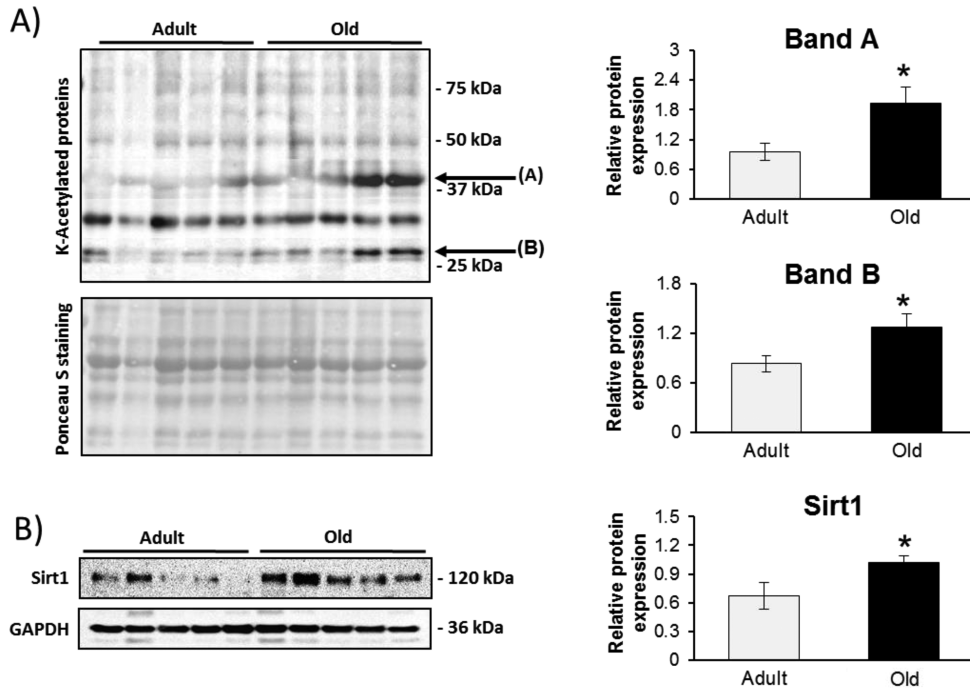
Figure 4. (A) Global lysine acetylation levels were analyzed in gastrocnemius muscles from adult and old mice using an anti-acetyl lysine antibody. (B) Immunoblot showing an increase in Sirt1 expression with aging.
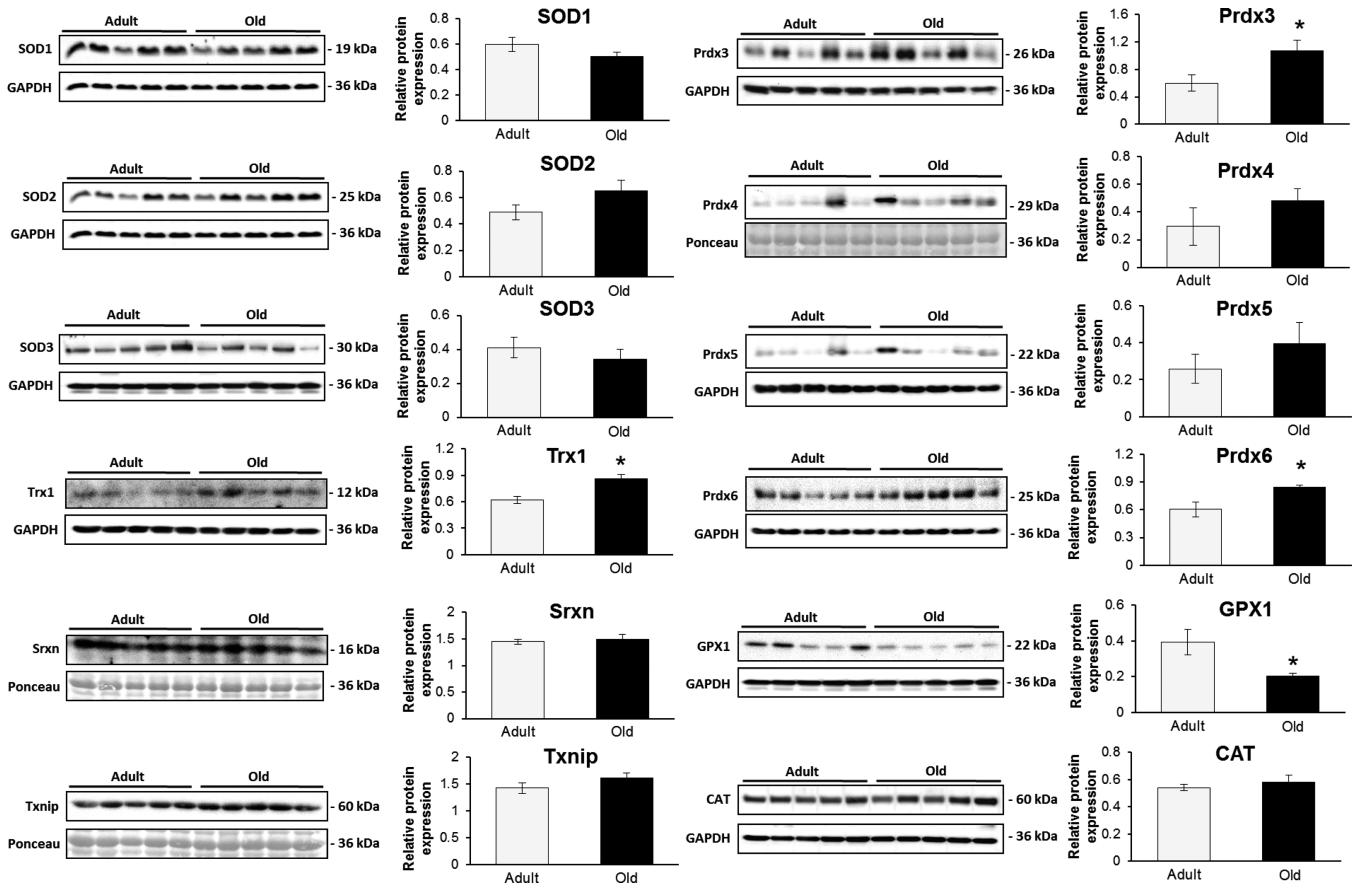
Figure 5. Immunoblotting for a number of proteins involved in direct and indirect regulation of superoxide and hydrogen peroxide. Sirt1 is a regulator of a number of FOXO3-dependent antioxidant proteins including SOD2, Gpx1, Prdx3, and Prdx5.

(Figure 4B), which may indicate an activation of antioxidant stress response in samples from old mice. Deacetylation of the

transcription factor FOXO3 by Sirt1 has been linked with the transcription of many antioxidant genes including MnSOD

Figure 6. (A) Representative extracted ion chromatograms (XIC) and fragmentation of aconitase peptide [380]VGILSCTNNSSYEDMGR[396] from a single MS analysis. The ratio of Cys385 in the reduced and reversibly oxidized state can be estimated from the intensity of the parent ions of the peptide with C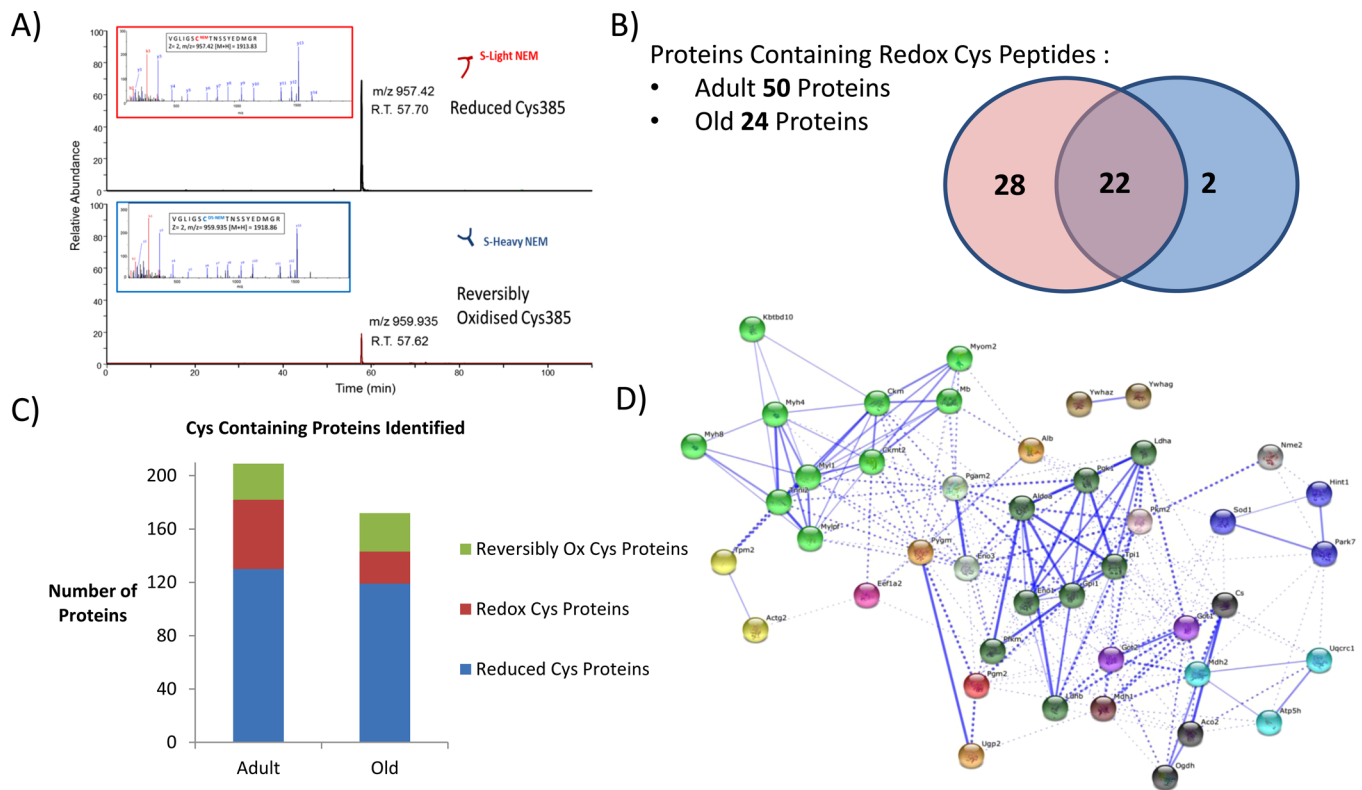ys-d0-NEM (reduced) and Cys-d5-NEM (reversibly oxidized). Identified peptides containing redox Cys residues are quantified with Skyline using both retention times and m/z values. (B) The number of proteins identified from peptides containing Cys; the number of proteins identified with redox peptides decreases with aging from 50 to 24. Overlapping circles show those proteins present in muscles from adult (pink) and old (blue) mice. Twenty two of the redox proteins were present in mucle samples from both groups. (C) Number of proteins identified containing reduced Cys only (blue), reversibly oxidized Cys only (green), and redox Cys peptides (red). (D) String analysis of identified proteins containing redox Cys residues from both groups, enriched for proteins involved in generation of precursor metabolites and energy ($p = 4.72 \times 10^{-20}$). Thicker lines represent stronger associations.

(SOD2), catalase (Cat), glutathione peroxidase 1 (Gpx1), and peroxiredoxins 3 (Prdx3) and 5 (Prdx5).[28] Figure 5 presents immunoblots to quantify the protein expression of some Sirt1-regulated proteins and related regulatory enzymes involved in H_2O_2 and superoxide detoxification including catalase, SOD1−3, Gpx1, Prdx3 and 5. Most of the immunoblots confirm the label-free proteomic results and indicate no specific increase in many of the stress response proteins. Trx1 had a significantly higher expression according to the immunoblot, although the label-free proteomic results did not reach significance. Trx1 is involved in the catalytic cycle of the 2-cys peroxiredoxins, resulting in reversible oxidation of its catalytic site Cys residues, and can induce apoptosis. Prdx3 and Prdx6 showed increased expression in samples from old mice, but Prdx5 did not (Figure 5). Sulforedoxin (Srxn), which can reduce the peroxidatic Cys within the active site of 2-cys prx's when oxidized to a sulfinic acid, showed no difference in expression between samples from adult and old mice (Figure 5). Similarly, thioredoxin interacting protein (Txnip), also known as vitamin D3 upregulated protein 1 (Vdup1), showed no significant changes between the muscles from adult and old mice. Txnip is associated with oxidative stress through its interaction with Trx1 and has also been shown to be associated with high glucose and catabolism of branched chain amino acids.[29,30]

Redox Analysis of Skeletal Muscle Cys-Containing Proteins from Adult and Old Mice

Differential labeling of reduced and reversibly oxidized Cys residues in proteins allowed a global view of the reduced and reversibly oxidized redox proteome within mouse skeletal muscle. Taking the identified peptide from the Mascot search results, the proteins identified were grouped into those with peptides containing only d(0) NEM modification (or reduced Cys residues), those proteins containing only d(5) NEM modification (or reversibly oxidized Cys residues), and those proteins that contained redox peptides, i.e., identical peptides identified independently with both d(0) and d(5) NEM modifications (redox Cys residues Figure 6A). In the adult mice, we identified 207 Cys-containing proteins, with 130 proteins detected with reduced Cys residues only (individual proteins and the Cys peptides are included in Supporting Information file 5), 27 with oxidized Cys residues only (Supporting Information file 6), and 50 proteins containing redox Cys residues (Supporting Information file 7). In the samples from old mice, 172 proteins were detected with Cys residues, of which 119 had reduced Cys residues (Supporting Information file 8), 29 with reversibly oxidized Cys residues (Supporting Information file 9), and 24 with redox Cys residues (Figure 6B,C and Supporting Information file 10). It is clear even from this crude analysis that skeletal muscle aging is associated with an altered redox state. Of the 24 redox-

Table 1. List of Proteins Containing Redox-Sensitive Cys Residues Detected by the Redox Proteomic Approach[a]

accession	protein	adult vs aged	(−log₁₀ P)	redox Cys	adult red/ox	old red/ox
P63101	14-3-3 protein zeta/delta (Ywhaz)	1.32:1.00	8.88	Cys94	2.35	0.772
P61982	14-3-3 protein gamma (Ywhag)	1.24:1.00	6.97	Cys112	18.98	100
P47857	6-Phosphofructokinase, muscle type (Pfkm)	1.44:1.00	13.77	Cys709	10.3	15.6
				Cys351	3.01	3.98
Q99KIO	Aconitate hydratase, mitochondrial (Aco2)	1.05:1.00	5.61	Cys126	4.76	7.414
				Cys385	2.38	3.62
				Cys448/451**	1.77	19.01
P68134	**Actin, alpha skeletal muscle (Actal)**	**0.58:1.00**	**25.79**	Cys219	9.52	11.44
				Cys259	5.18	9.17
				Cys287	10.71	18.83
P07724	Serum albumin (Alb)	1.24:1.00	11.6	Cys58	1.46	1.37
				Cys77	0.0045	0.00026
				Cys289	0.0071	0.0053
				Cys500/501**	0.002	0.003
				Cys703	1.12	1.97
088990	Alpha-actinin-3 (Actn3)	0.34:1.00	18.14	Cys868	4.85	4.28
P05201	Aspartate aminotransferase, cytoplasmic (Gotl)	1.17:1.00	7.5	Cys391	10.58	26.43
P05202	Aspartate aminotransferase, mitochondrial (Got2)	1.10:1.00	6.86	Cys106	18.95	28.54
				Cys187	0.866	0.093
				Cys295	2.45	2.14
P16015	Carbonic anhydrase 3 (Ca3)	1.07:1.00	6.04	Cysl82/187*	33.11	0.194
Q9CZU6	Citrate synthase, mitochondrial (Cs)	1.21:1.00	9.83	Cys359	7.9	11.28
P45591	Cofilin-2 (Cfl2)	1.11:1.00	7.06	Cys80	34.44	67.18
P07310	Creatine kinase M-type (Ckm)	1.46:1.00	17.2	Cys146	7.41	7.01
				Cys254	77.04	30.12
Q6P8J7	Creatine kinase S-type, mitochondrial (Ckmt2)	1.38:1.00	12.27	Cys180	4.69	6.86
				Cys238	9.38	11.48
				Cys317	12.55	24.72
P62631	Elongation factor 1-alpha 2 (Eef1a2)	1.09:1.00	6.29	Cys326	12.17	18.14
P21550	Beta-enolase (Eno3)	1.40:1.00	16.08	Cys337/339*	191.5	114.3
				Cys389	12.66	20.24
				Cys399	11.4	16.51
P05064	Fructose-bisphosphate aldolase A (Aldoa)	1.37:1.00	19.33	Cys73	7.85	7.63
				Cysl35	8.15	8.12
				Cys178	4.94	7.73
				Cys202	18.64	12.9
				Cys290	7.66	16.68
				Cys339	10.83	16.93
P06745	Glucose-6-phosphate isomerase (Gpi)	1.26:1.00	8.4	Cysl33	7.72	6.76
				Cys404	8.46	4.75
P16858	**Glyceraldehyde-3-phosphate dehydrogenase (Gapdh)**	**4.64:1.00**	**81.41**	Cys22	42.19	47.76
				Cys150/154*	38.81	9.15
				Cys245	18.15	11.33
Q9WUB3	**Glycogen phosphorylase, muscle form (Pygm)**	**1.92:1.00**	**21.12**	Cys172	45.85	135.8
				Cys373	2.899	0.702
				Cys496	25.91	41.06
Q99ME9	Nucleolar GTP-binding protein 1 (Gtpbp4)	0.97:1.00	6.02	Cys336	0.63	1.69
P63017	Heat shock cognate 71 kDa protein (Hspa8)	1.29:1.00	10.21	Cys267	21.4	14.99
				Cys603	13.19	26.49
P70349	Histidine triad nucleotide-binding protein 1 (Hintl)	0.99:1.00	5.26	Cys38	2.25	6.54
P06151	**L-lactate dehydrogenase A chain (Ldha)**	**1.62:1.00**	**24.66**	Cys84	22.63	26.33
				Cys163	12.99	21.44
P51174	Long-chain specific acyl-CoA dehydrogenase, mitochondrial (Acadl)	1.03:1.00	5.15	Cys166	14.55	13.59
				Cys351	16.21	8.48
P14152	Malate dehydrogenase, cytoplasmic (Mdhl)	1.29:1.00	10.52	Cys137	15.31	18.61
				Cys154	20.34	13.59
P08249	Malate dehydrogenase, mitochondrial (Mdh2)	1.24:1.00	9.81	Cys89	6.83	10.93
				Cys93	11.08	24.99
Q9DCX2	ATP synthase subunit d mitochondrial (Atp5h)	1.37:1.00	6.48	Cys101	16.67	4.36
P04247	Myoglobin (Mb)	0.93:1.00	7.64	Cys67	12.92	26.8
Q5SX39	**Myosin-4 (Myh4)**	**1.59:1.00**	**23.88**	Cys796	2.31	6.47

Table 1. continued

accession	protein	adult vs aged	$(-\log_{10} P)$	redox Cys	adult red/ox	old red/ox
				Cys817	9.94	10.16
				Cys1344	7.76	24.07
				Cys1443	1.23	0.049
P97457	**Myosin regulatory light chain 2, skeletal muscle isoform (Mylpf)**	**0.59:1.00**	**23.8**	Cys128	6.85	6.96
				Cys157	1.54	0.1043
P05977	**Myosin light chain 1/3, skeletal muscle isoform (Myl1)**	**0.57:1.00**	**22.26**	Cys62	30.75	83.28
Q91YTO	NADH dehydrogenase [ubiquinone] flavoprotein 1, mitochondrial	0.86:1.00	4.33	Cys127	5.33	10.37
Q01768	Nucleoside diphosphate kinase B (Nme2)	1.39:1.00	7.31	Cys109	16.62	26.22
				Cys145	9.26	12.91
P17742	**Peptidyl-prolyl cis−trans isomerase A (Ppia)**	**1.96:1.00**	**23.34**	Cys161	7.56	6.16
Q9D0F9	**Phosphoglucomutase-1 (Pgml)**	**1.60:1.00**	**22.56**	Cys160	50.33	32.61
				Cys374	22.65	53.12
P09411	**Phosohoglycerate kinase 1 (Pgkl)**	**3.12:1.00**	**67.17**	Cys379/380*	32.69	31.7
O70250	**Phosphoglycerate mutase 2 (Pgam2)**	**4.18:1.00**	**91.19**	Cys23	21.96	95.46
				Cys153	2.105	0.306
Q99LXO	**Protein DJ-1 (Park7)**	**2.31:1.00**	**32.32**	Cys53	42.05	53.66
P52480	Pyruvate kinase isozymes M1/M2 (Pkm2)	1.43:1.00	15.87	Cys49	10.98	35.88
				Cys358	10.32	18.14
				Cys474	16.88	93.68
Q921I1	Serotransferrin (Tf)	1.05:1.00	6.28	Cys683	0.016	0.03
P08228	Superoxide dismutase [Cu−Zn] (Sodl)	1.21:1.00	9	Cys796	0.83	0.48
				Cys147	0.54	0.34
				Cys220	0.711	ND
P17751	Triosephosphate isomerase (Tpi 1)	1.44:1.00	18.54	Cys117	11.94	51.84
				Cys177	15.03	24.62
				Cys268	4.73	5.84
P58771	Tropomyosin alpha-1 chain (Tpml)	0.95:1.00	9.59	Cys190	9.56	19.4
P58774	Tropomyosin beta chain (Tpm2)	0.93:1.00	8.23	Cys36	11.72	7.91
				Cys190	8.51	5.29
P13412	Troponin I, fast skeletal muscle (Tnni2)	0.77:1.00	11.64	Cys134	10.26	19.46

[a]The table includes label-free quantification of the protein from PEAKS 7 analysis and the redox ratio of individual Cys residues within those proteins. The redox state of selected redox Cys residues labeled with both d(0) NEM and d(5) NEM was calculated using the ratio of the average ion intensity of parent ions. The m/z values and retention times of selected peptides were applied in the targeted approach using Skyline open software. Proteins highlighted in bold have a significant change in abundance between muscle samples from adult and old mice, and * indicates a tryptic peptide containing two cysteine residues.

containing proteins, 22 of these were also detected in samples from adult mice; interestingly, the 2 proteins detected only from old muscle samples with redox peptides were cytoskeletal regulatory proteins cofilin-2 (Cys80) and α-actinin 3 (Cys868).

Proteins that were identified as containing redox-sensitive Cys residues in adult samples only, included many proteins involved in glucose metabolism (Figure 6D) such as phosphofructokinase, glucose 6-phosphate isomerase, glycogen phosphorylase, phophoglycerate mutase 1, and phosphoglucomutase 2 (Table 1). Many of these proteins require Cys residues for their activity, and this suggests muscle from adult mice has greater flexibility in the metabolic redox response. Peptidyl-prolyl isomerase A (Ppia), heat shock cognate 71 (Hspa8), and Parkinson disease 7 (Park7) were detected as containing redox Cys residues only in samples from adult mice, although the expression levels of Ppia (1.96:1.00, $-\log(P)$ = 23.34) and Park7 (2.31:1.00, $-\log(P)$ = 32.32) were also higher in the samples from adult animals. Park7 has previously been reported in vivo and in vitro to be a target of S-nitrosylation that can regulate its activity,[31] and our results indicate Cys53 as being redox-sensitive (Table 1) and Cys106 and Cys121 in the reduced state.

Targeted Analysis and Quantification of Redox Peptides Detected from Adult and Old Mice

Identical peptides identified from fragmentation of parent ions with d(0) NEM and d(5)NEM modifications independently from the Mascot search results were considered redox peptides, as outlined in Experimental Methods, i.e., individual peptide ion score > 20 and identified with both d(0) and d(5) NEM modifications independently. The m/z values and retention times of identified redox peptides were utilized for a targeted redox quantification analysis of the parent ion intensity with Skyline. Application of such stringent criteria resulted in 91 Cys-containing peptides from 46 proteins selected for targeted quantification of their individual redox state. The retention time and fragmentation spectra of these peptides were employed to perform a targeted LC−MS analysis to calculate the ratio of the reversible oxidation state of the individual Cys peptides and provide an indication of the redox-sensitive Cys residues within those proteins. Table 1 lists the proteins and includes relative protein abundance and significance value between muscles from adult and old mice, the redox Cys residues within those proteins, and the average ratio intensity d(0)/d(5) NEM modified peptides (ratio of reduced/reversibly oxidized Cys residues). It should be noted that since this method uses the intensity of the parent ion for an indication of the redox state of individual Cys residues, the analysis of peptides containing two
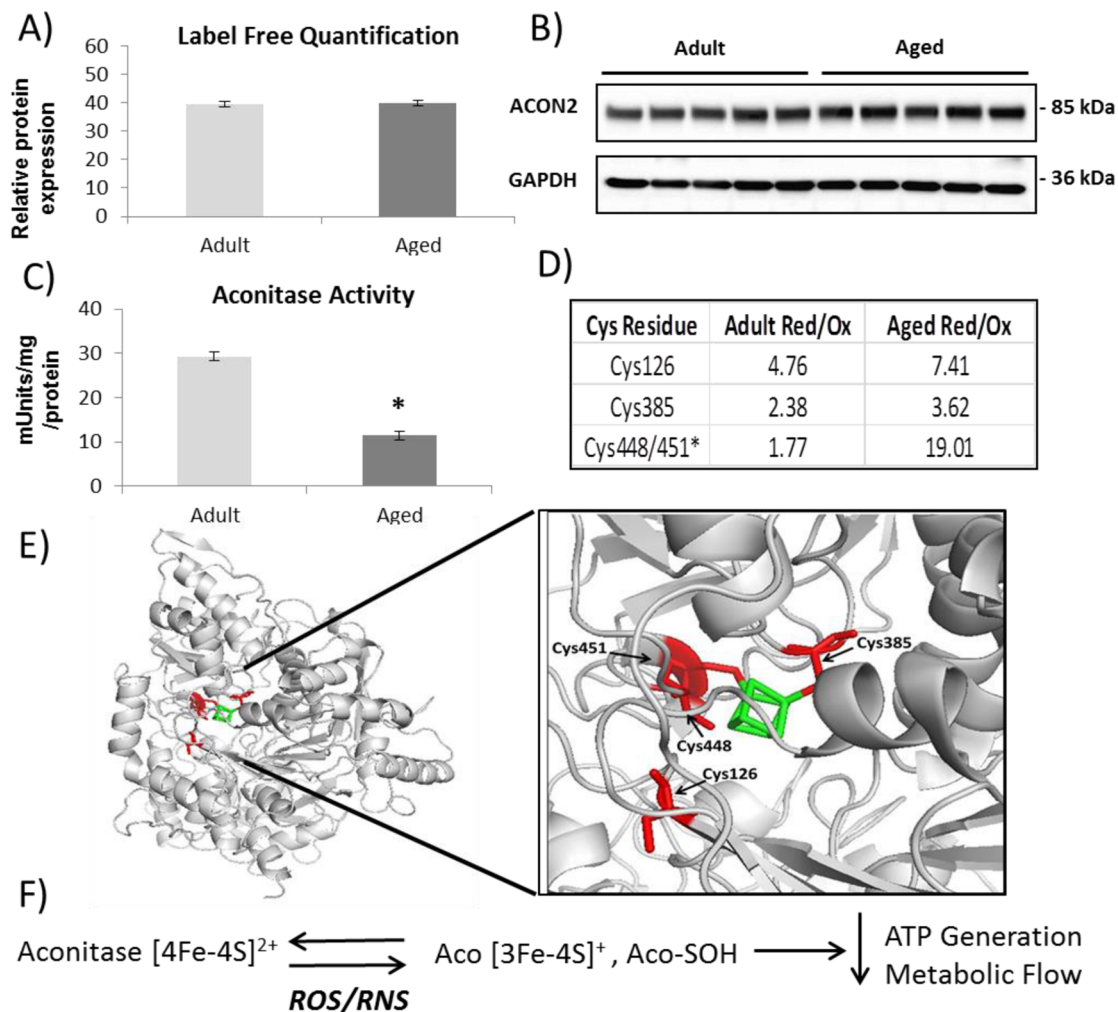
Figure 7. Proteomic and redox analysis of aconitase from gastrocnemius muscle of adult and old mice. (A) PEAKS label-free proteomic quantification of aconitase from a shotgun proteomics of gastrocnemius muscle from adult and old mice. (B) Western blotting validation of aconitase expression. (C) Aconitase enzymatic activity showing a decrease in muscle from old mice. (D) Redox quantification using Skyline of reversible oxidation state of individual Cys residues. (E) Structure of aconitase with Cys residues detected and quantified (red) and coordinating iron (green). (F) Schematic of aconitase oxidation.

Cys residues where there is potential oxidation of either or both residues makes the analysis more complicated. Previously, we demonstrated with selective MS/MS ion monitoring (SMIM) of a peptide containing two Cys residues from alcohol dehydrogenase treated in vitro with H_2O_2 that it could exist in, potentially, 12 different oxidation states.[32] In these examples, it is necessary to examine individually the MS/MS results to identify the redox-sensitive Cys. Of the 46 proteins, we selected two well-characterized redox proteins, aconitase[33] and fructose bisphosphate aldolase A,[34] for further analysis.

Redox Proteomic Analysis of Aconitase in Skeletal Muscle from Adult and Old Mice

The enzymatic activity of the redox-sensitive and Fe−S cluster protein aconitase is often used as an indicator of superoxide generation within the mitochondria and general mitochondrial health. Analysis of the redox proteomic results suggests that the protein exists in an altered redox state with the four Cys residues contained within three tryptic peptides that coordinate iron detected in altered reversible oxidation states between samples (Figure 7D). The activity of the enzyme is significantly downregulated in aging (Figure 7C) even though protein levels are unchanged (Figure 7A,B), indicating that the redox status of

the Cys residues coordinating iron significantly affects the activity of the protein.

Redox Regulation of Fructose Bisphosphate Aldolase

Fructose bisphosphate aldolase A (Aldoa), a redox-sensitive protein, has been previously identified as being glutathionylated and nitrosylated, resulting in partial and reversible inactivation of the enzyme.[34] Binding of fructose bisphosphate or redox modifications of Cys residues can cause conformational changes in the protein, affecting activity.[34] In our proteomic screen, we detected six redox Cys residues within the protein, and we observed a trend for the protein to be downregulated in samples from old mice. The published structure of Aldoa is a tetramer, and Figure 8A indicates the structure and the positioning of the Cys residues within the tetramer. Our redox screen suggests that aging results in the increased reversible oxidation of, predominantly, Cys202 positioned close to the active site (Figure 8B,C), whereas examination of the structure indicates Cys73−Cys339 and Cys135−Cys178 could potentially form disulfide bonds (Figure 8B).
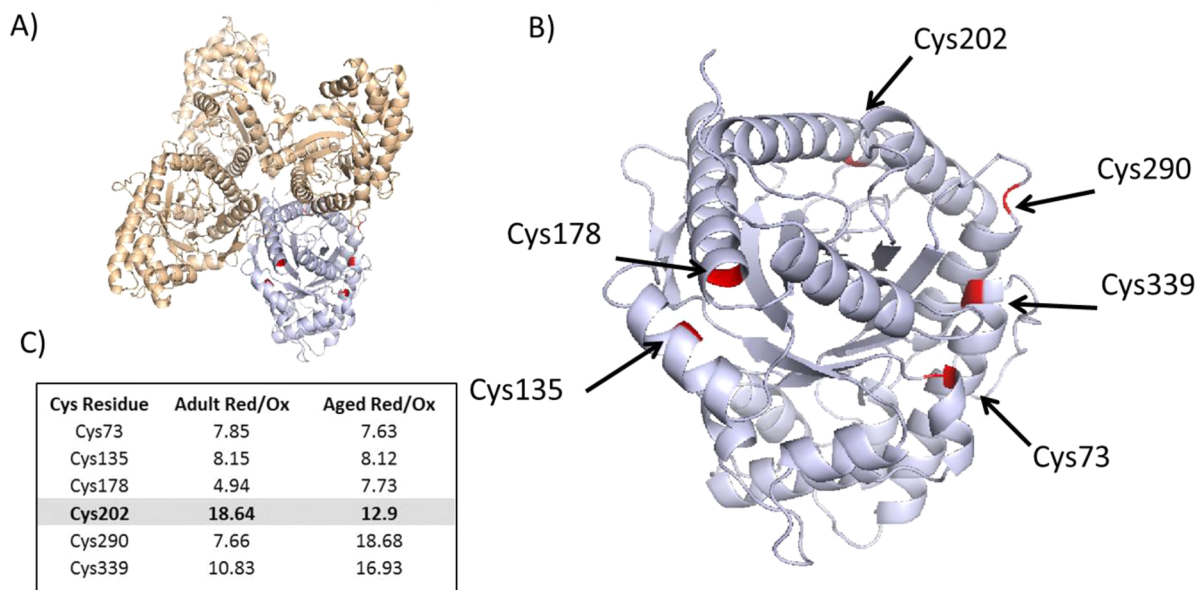
Cys Residue	Adult Red/Ox	Aged Red/Ox
Cys73	7.85	7.63
Cys135	8.15	8.12
Cys178	4.94	7.73
Cys202	18.64	12.9
Cys290	7.66	18.68
Cys339	10.83	16.93

Figure 8. Redox regulation of fructose bisphosphate aldolase (Aldoa). (A) Tetramer of Aldoa (PDB ID: 3B8D), with Cys residues detected and highlighted in monomer. (B) Monomer of Aldoa with redox Cys detected and highlighted. (C) Relative quantification of redox-sensitive Cys residues detected; ratios represent an average of the ratio of the reduced and reversibly oxidized Cys residues.

■ DISCUSSION

Cysteine residues demonstrate an extreme diversity in their pattern of conservation: highly conserved in functional and catalytic positions but poorly conserved otherwise.[35] As Cys can occupy a number of oxidation states, it is highly adapted to the dynamic nature of the proteome, allowing the cell to respond rapidly to environmental, biochemical, and pathological conditions through reversible oxidative modification of key residues. There has been a lot of interest in implementing techniques that (i) allow the identification of redox susceptible Cys residues within proteins and (ii) can quantify the redox state of individual Cys residues.[36,37] A number of redox proteomic studies have quantified the reduced and reversibly oxidized state of individual Cys residues within a protein sample, but these rely on purifying and identifying the Cys-containing peptides, and information on overall protein abundance is lost.[32,38−40] In the present study, we have utilized the light and heavy isotopic form of a common laboratory reagent NEM to differentially and irreversibly label the reduced and reversibly oxidized forms of the Cys residues. The overall protein abundance can be relatively quantified between samples from the intensity of tryptic peptides unique to the particular protein. This technique adds an extra dimension to the proteomic experiment, allowing identification of not only the proteins that are up/downregulated but also to identify and quantify the redox state of specific sensitive Cys residues within those proteins. As this technique generates information on both overall protein abundance and individual Cys reversible oxidation state, the major disadvantage in comparison to techniques that purify modified Cys peptides is a loss in sensitivity for the detection of low-abundance proteins. Also, techniques that employ iTRAQ or, similarly, TMT (tandem mass tags) can analyze a number of samples simultaneously, reducing any LC−MS/MS run variability.[41]

Skeletal muscle consumes a large portion of the ATP within the body and requires a certain level of ROS/RNS for optimal contractions and the adaptive response to exercise. Muscle fibers can be broadly divided into slow twitch or type I and fast or type II fibers. Type I fibers predominantly generate ATP as a result of oxidative phosphorylation, whereas type II fibers produce energy by a mixture of glycolytic/oxidative metabolism, which could have important consequences for the species and concentration of ROS/RNS generated by the fiber type and subsequently the redox proteome. Skeletal muscle is unique in that there are a number of ROS/RNS generating systems within the muscle fibers, including NOX and NOS enzymes,[42] whose activity needs to be tightly regulated for optimal muscle function.[6]

Global indicators of oxidative stress demonstrate an increase in irreversible protein modifications as revealed by carbonylation but not excessive oxidative damage in samples from old mice and a similar expression of the NOS enzymes in adult and old muscle samples. Label-free proteomic analysis indicated an increased expression of glycolytic and chaperone/heat shock proteins in muscle from adult mice compared to that from old mice, whereas aging induced a higher expression of a number of core histones. We confirmed the altered expression of a number of proteins by immunoblotting and proteins that were acetylated on Lys residues. The class III NAD⁺-dependent deacetylase Sirt1 is responsible for the regulation of transcription of a number of key histone but also non-histone targets including transcription factors and essential proteins involved in the antioxidant response, e.g., p53, FOXO1/3, peroxisome proliferator activated receptor gamma coactivator (PGC-1α), and nuclear factor (NF)-κB.[43] These transcription factors control the expression of a large number of antioxidant proteins that are thought to play a key role in the aging process. Sirt1 expression has been linked with the fasted state in caloric restriction, which is associated with activation of AMPK to generate ATP and helps control cellular energy homeostasis.[44] We found an increased expression of Sirt1 from old mice and an increase in only Prdx3 of the FOXO3-regulated proteins[28] (Figure 5). The reduced expression of the α-catalytic subunit of AMPK (Prkar2a) seen in the label-free proteomic analysis in addition to the lack of alteration in the expression of most of the H_2O_2 and superoxide metabolizing antioxidant enzymes

support a chronic activation of Sirt1 in aged skeletal muscle. There was also a reduction in adenylate kinase (Ak1), a key regulator of cellular ATP levels catalyzing the interconversion between 2ADP ↔ ATP + AMP, influencing AMP signaling and also AMP dependent AMPK activation. AMPK activation has also been reported to be Trx-dependent[45] and to lead to the phosphorylation and degradation of Txnip.[46] Txnip can bind to and inhibit the action of thioredoxin, but it is also thought to play a role in energy homeostasis, controlling glucose uptake and maintenance of specific mitochondrial dehydrogenases required for fuel switching such as during diauxic shift.[30] Moreover, protein DJ-1 or Park7, the Parkinson's associated protein, was found to be downregulated with age. This protein has been widely associated with neurodegenerative disorders and is considered to be a multifunctional protein associated with the mitochondrial autophagic and oxidant stress response.[47] This family of proteins has also been recently associated with diauxic shift in yeast[48] and may point to a crucial role of the protein within cancer cells and metabolic reprogramming in skeletal muscle. Cellular energy signaling is controlled by the balance of cell regulators, some of which have opposing effects, including AMPK and mammalian target of rapamycin (mTOR). Thus, the label-free quantitative proteomics experiments undertaken in the present study indicate that aging results in major changes in the glycolytic metabolic enzymes and also in the regulatory enzymes controlling energy homeostasis within skeletal muscle.

The redox proteomic approach undertaken allowed the identification and relative quantification of the oxidation state of specific Cys residues within redox-sensitive proteins and also included the label-free quantification of individual proteins. It is clear from the redox results muscle samples from old mice have a reduced redox flexibility compared to the muscle samples from adult mice (Figure 6), but interestingly, two redox proteins were detected only in old mice: cofilin-2 and actinin-3. The reversible oxidation status of Cys residues on non-muscular cofilin has been linked to a pro-apoptotic signal and is essential for its regulatory effect on actin polymerization and depolymerization.[49] Cofilin-2, the isoform present in striated muscle, expression levels did not change between samples from adult and old mice (1.11:1.00), but Cys80 of cofilin-2 was detected as a redox residue in samples from old mice only. Actinin-3 is an F-actin binding proteins that is exclusively expressed in fast twitch muscle fibers and has been linked with muscle mass and glycogen utilization.[50] This protein is thought to sense tension during muscle contractions and link it with the signaling effect possibly through an interaction with calcineurin;[50] in this study, actinin-3 levels were trending higher in old mice (0.34:1.00, −log(P) = 18.14), and it was detected with a redox-regulated Cys868 residue in samples from old mice only. Both of these proteins were detected as redox-dependent proteins only in samples from old mice, suggesting a dysregulation of the cytoskeletal regulatory proteins in old muscle.

For the targeted analysis of redox peptides, stringent criteria was applied for the selection of the redox peptides. The technique has identified and quantified redox-sensitive Cys residues in 91 tryptic peptides from 46 proteins, enriched for proteins involved in the generation of precursor metabolites and energy. The advantage of the technique developed in this study is highlighted by the detailed examination of aconitase. Aconitase, an essential protein of the mitochondrial TCA cycle, has another cytosolic function as an iron regulatory protein 1

(Irp1) to bind and stabilize ferritin mRNA. Label-free and immunoblotting results demonstrate that aconitase abundance does not change with aging but its activity is dramatically reduced in muscle from old mice. We identified the three tryptic peptides that contain the four Cys residues that coordinate the iron atom necessary for activity, and the redox analysis indicates that muscle from old mice had an increase in the proportion of these residues in the reduced state, which would affect the activity of the protein. In a standard quantitative proteomic approach, this information would be lost, and, similarly, if only Cys-containing peptides were analyzed, then we would detect changes in the oxidative state of the proteins without information on the overall protein abundance. This highlights the major advantage of the current approach over a traditional quantitative proteomics, which does not give information on the functional proteome. Cross-talk between post-translational modifications has been clearly defined in the oxidative regulation of kinases and phosphatases.[51] In this study, we analyzed the reversible oxidation of Cys residues, but one of the remaining challenges is the integration of numerous PTMs and their effects on protein activity in the functional proteome.

CONCLUSIONS

ROS/RNS generated by skeletal muscle are involved in a coordinated local response tightly controlled at all levels from generation to detoxification. Our results indicate that during aging mouse muscle shows a decreased expression of many glucose metabolic enzymes and essential chaperone proteins, whereas there is an increased expression of ER stress response proteins and histones. The redox analyses of skeletal muscle from adult and old mice clearly demonstrates a decrease in redox-responsive proteins in aged skeletal muscle and implies a reduced flexibility in the redox proteome response. The long-term physiological consequences of impaired redox signaling and chronic activation of key proteins in aged skeletal muscle will potentially be particularly important in the metabolic response to altered ROS/RNS generation in muscle fibers during exercise.

There are a number of metabolic and muscle disorders that are associated with aberrant redox regulation.[52,53] Dysregulated ROS homeostasis or signaling responses have been reported in a variety of human skeletal muscular dystrophies,[53] cancers,[54] neurodegeneration,[15] obesity,[55] and, increasingly, metabolic disease such as diabetes.[56] The redox proteomic approach developed in the present study could be readily applied to these disorders to identify metabolic pathways that are affected. This technique provides meaningful information regarding the overall proteome and both the sensitivity and oxidation states of individual cysteine residues.

ASSOCIATED CONTENT

Ⓢ Supporting Information

File 1 (.docx): Data analysis, results and search parameters for MS/MS data. File 2 (.xlsx): LC−MS data for proteins that change significantly between muscle samples from adult and old mice. File 3 (.xlsx): Acetylated proteins in adult and old mice and fragmentation spectra of acetylated peptide from Histone H3. File 4 (.xlsx): Skyline quantification results of targeted redox peptides. File 5 (.xlsx): Proteins detected from adult mouse skeletal muscle with reduced Cys residues only. File 6 (.xlsx): Proteins detected from adult mouse skeletal

muscle containing reversibly oxidized Cys residues only. File 7 (.xlsx): Proteins detected from adult mouse skeletal muscle containing redox sensitive Cys residues. File 8 (.xlsx): Proteins detected in skeletal muscle from old mice containing reduced Cys residues only. File 9 (.xlsx): Proteins detected from old mouse skeletal muscle containing reversibly oxidized Cys residues only. File 10 (.xlsx): Proteins detected from old mouse skeletal muscle containing redox sensitive Cys residues. This material is available free of charge via the Internet at http://pubs.acs.org.

■ AUTHOR INFORMATION

Corresponding Author

*Phone: +44 151 7064124. Fax: +44 1517065802. E-mail: b. mcdonagh@liverpool.ac.uk.

Notes

The authors declare no competing financial interest.

■ ACKNOWLEDGMENTS

■ ABBREVIATIONS

AMPK, cAMP dependent protein kinase; NEM, *N*-ethylmaleimide; NOX, NADP(H) oxidase; NOS, nitric oxide synthase; RNS, reactive nitrogen species; ROS, reactive oxygen species

■ REFERENCES

(1) Close, G. L.; Ashton, T.; McArdle, A.; Jackson, M. J. Microdialysis studies of extracellular reactive oxygen species in skeletal muscle: factors influencing the reduction of cytochrome c and hydroxylation of salicylate. *Free Radical Biol. Med.* **2005**, *39*, 1460−7.

(2) Vasilaki, A.; Mansouri, A.; Van Remmen, H.; van der Meulen, J. H.; Larkin, L.; Richardson, A. G.; McArdle, A.; Faulkner, J. A.; Jackson, M. J. Free radical generation by skeletal muscle of adult and old mice: effect of contractile activity. *Aging Cell* **2006**, *5*, 109−17.

(3) Powers, S. K.; Jackson, M. J. Exercise-induced oxidative stress: cellular mechanisms and impact on muscle force production. *Physiol. Rev.* **2008**, *88*, 1243−76.

(4) Sun, Q. A.; Wang, B.; Miyagi, M.; Hess, D. T.; Stamler, J. S. Oxygen-coupled redox regulation of the skeletal muscle ryanodine receptor/Ca^{2+} release channel (RyR1): sites and nature of oxidative modification. *J. Biol. Chem.* **2013**, *288*, 22961−71.

(5) Tong, X.; Hou, X.; Jourd'heuil, D.; Weisbrod, R. M.; Cohen, R. A. Upregulation of Nox4 by TGF*β*1 oxidizes SERCA and inhibits NO in arterial smooth muscle of the prediabetic Zucker rat. *Circ. Res.* **2010**, *107*, 975−83.

(6) Sakellariou, G. K.; Jackson, M. J.; Vasilaki, A. Redefining the major contributors to superoxide production in contracting skeletal muscle. The role of NAD(P)H oxidases. *Free Radical Res.* **2014**, *48*, 12−29.

(7) Labunskyy, V. M.; Gladyshev, V. N. Role of reactive oxygen species-mediated signaling in aging. *Antiox. Redox Signaling* **2012**, *19*, 1362−72.

(8) Egan, B.; Zierath, J. R. Exercise metabolism and the molecular regulation of skeletal muscle adaptation. *Cell Metab.* **2013**, *17*, 162−84.

(9) Aachmann, F. L.; Sal, L. S.; Kim, H. Y.; Marino, S. M.; Gladyshev, V. N.; Dikiy, A. Insights into function, catalytic mechanism, and fold evolution of selenoprotein methionine sulfoxide reductase B1 through structural analysis. *J. Biol. Chem.* **2010**, *285*, 33315−23.

(10) Anastasiou, D.; Poulogiannis, G.; Asara, J. M.; Boxer, M. B.; Jiang, J. K.; Shen, M.; Bellinger, G.; Sasaki, A. T.; Locasale, J. W.; Auld, D. S.; Thomas, C. J.; Vander Heiden, M. G.; Cantley, L. C. Inhibition of pyruvate kinase M2 by reactive oxygen species contributes to cellular antioxidant responses. *Science* **2011**, *334*, 1278−83.

(11) Murphy, M. P.; Holmgren, A.; Larsson, N. G.; Halliwell, B.; Chang, C. J.; Kalyanaraman, B.; Rhee, S. G.; Thornalley, P. J.; Partridge, L.; Gems, D.; Nystrom, T.; Belousov, V.; Schumacker, P. T.; Winterbourn, C. C. Unraveling the biological roles of reactive oxygen species. *Cell Metab.* **2011**, *13*, 361−6.

(12) Sakai, J.; Li, J.; Subramanian, K. K.; Mondal, S.; Bajrami, B.; Hattori, H.; Jia, Y.; Dickinson, B. C.; Zhong, J.; Ye, K.; Chang, C. J.; Ho, Y. S.; Zhou, J.; Luo, H. R. Reactive oxygen species-induced actin glutathionylation controls actin dynamics in neutrophils. *Immunity* **2012**, *37*, 1037−49.

(13) Requejo, R.; Hurd, T. R.; Costa, N. J.; Murphy, M. P. Cysteine residues exposed on protein surfaces are the dominant intramitochondrial thiol and may protect against oxidative damage. *FEBS J.* **2010**, *277*, 1465−80.

(14) Jones, D. P. Radical-free biology of oxidative stress. *Am. J. Physiol.: Cell Physiol.* **2008**, *295*, C849−68.

(15) Calabrese, V.; Sultana, R.; Scapagnini, G.; Guagliano, E.; Sapienza, M.; Bella, R.; Kanski, J.; Pennisi, G.; Mancuso, C.; Stella, A. M.; Butterfield, D. A. Nitrosative stress, cellular stress response, and thiol homeostasis in patients with Alzheimer's disease. *Antiox. Redox Signaling* **2006**, *8*, 1975−86.

(16) MacLean, B.; Tomazela, D. M.; Shulman, N.; Chambers, M.; Finney, G. L.; Frewen, B.; Kern, R.; Tabb, D. L.; Liebler, D. C.; MacCoss, M. J. Skyline: an open source document editor for creating and analyzing targeted proteomics experiments. *Bioinformatics* **2010**, *26*, 966−8.

(17) Zhang, J.; Xin, L.; Shan, B.; Chen, W.; Xie, M.; Yuen, D.; Zhang, W.; Zhang, Z.; Lajoie, G. A.; Ma, B. PEAKS DB: de novo sequencing assisted database search for sensitive and accurate peptide identification. *Mol. Cell. Proteomics* **2012**, *11*, M111.010587.

(18) Larkin, L. M.; Davis, C. S.; Sims-Robinson, C.; Kostrominova, T. Y.; Van Remmen, H.; Richardson, A.; Feldman, E. L.; Brooks, S. V. Skeletal muscle weakness due to deficiency of CuZn-superoxide dismutase is associated with loss of functional innervation. *Am. J. Physiol.: Regul., Integr. Comp. Physiol.* **2011**, *301*, R1400−7.

(19) Vizcaino, J. A.; Deutsch, E. W.; Wang, R.; Csordas, A.; Reisinger, F.; Rios, D.; Dianes, J. A.; Sun, Z.; Farrah, T.; Bandeira, N.; Binz, P. A.; Xenarios, I.; Eisenacher, M.; Mayer, G.; Gatto, L.; Campos, A.; Chalkley, R. J.; Kraus, H. J.; Albar, J. P.; Martinez-Bartolome, S.; Apweiler, R.; Omenn, G. S.; Martens, L.; Jones, A. R.; Hermjakob, H. ProteomeXchange provides globally coordinated proteomics data submission and dissemination. *Nat. Biotechnol.* **2014**, *32*, 223−6.

(20) McDonagh, B.; Sheehan, D. Redox proteomics in the blue mussel *Mytilus edulis*: carbonylation is not a pre-requisite for ubiquitination in acute free radical-mediated oxidative stress. *Aquat. Toxicol.* **2006**, *79*, 325−33.

(21) Lustgarten, M. S.; Jang, Y. C.; Liu, Y.; Muller, F. L.; Qi, W.; Steinhelper, M.; Brooks, S. V.; Larkin, L.; Shimizu, T.; Shirasawa, T.; McManus, L. M.; Bhattacharya, A.; Richardson, A.; Van Remmen, H. Conditional knockout of Mn-SOD targeted to type IIB skeletal muscle fibers increases oxidative stress and is sufficient to alter aerobic exercise capacity. *Am. J. Physiol.: Cell Physiol.* **2009**, *297*, C1520−32.

(22) Huang, D. W.; Sherman, B. T.; Lempicki, R. A. Systematic and integrative analysis of large gene lists using DAVID bioinformatics resources. *Nat. Protoc.* **2009**, *4*, 44−57.

(23) Jensen, L. J.; Kuhn, M.; Stark, M.; Chaffron, S.; Creevey, C.; Muller, J.; Doerks, T.; Julien, P.; Roth, A.; Simonovic, M.; Bork, P.; von Mering, C. STRING 8—a global view on proteins and their functional interactions in 630 organisms. *Nucleic Acids Res.* **2009**, *37*, D412−6.

(24) Pfaffenbach, K. T.; Lee, A. S. The critical role of GRP78 in physiologic and pathologic stress. *Curr. Opin. Cell Biol.* **2011**, *23*, 150–6.

(25) Ralat, L. A.; Manevich, Y.; Fisher, A. B.; Colman, R. F. Direct evidence for the formation of a complex between 1-cysteine peroxiredoxin and glutathione S-transferase pi with activity changes in both enzymes. *Biochemistry* **2006**, *45*, 360–72.

(26) Ray, P. S.; Martin, J. L.; Swanson, E. A.; Otani, H.; Dillmann, W. H.; Das, D. K. Transgene overexpression of alphaB Crystallin confers simultaneous protection against cardiomyocyte apoptosis and necrosis during myocardial ischemia and reperfusion. *FASEB J.* **2001**, *15*, 393–402.

(27) Shao, D.; Fry, J. L.; Han, J.; Hou, X.; Pimentel, D. R.; Matsui, R.; Cohen, R. A.; Bachschmid, M. M. A redox-resistant sirtuin-1 mutant protects against hepatic metabolic and oxidant stress. *J. Biol. Chem.* **2014**, *289*, 7293–306.

(28) Olmos, Y.; Sanchez-Gomez, F. J.; Wild, B.; Garcia-Quintans, N.; Cabezudo, S.; Lamas, S.; Monsalve, M. SirT1 regulation of antioxidant genes is dependent on the formation of a FoxO3a/PGC-1α complex. *Antiox. Redox Signaling* **2013**, *19*, 1507–21.

(29) Shah, A.; Xia, L.; Goldberg, H.; Lee, K. W.; Quaggin, S. E.; Fantus, I. G. Thioredoxin-interacting protein mediates high glucose-induced reactive oxygen species generation by mitochondria and the NADPH oxidase, Nox4, in mesangial cells. *J. Biol. Chem.* **2013**, *288*, 6835–48.

(30) DeBalsi, K. L.; Wong, K. E.; Koves, T. R.; Slentz, D. H.; Seiler, S. E.; Wittmann, A. H.; Ilkayeva, O. R.; Stevens, R. D.; Perry, C. G.; Lark, D. S.; Hui, S. T.; Szweda, L.; Neufer, P. D.; Muoio, D. M. Targeted metabolomics connects thioredoxin-interacting protein (TXNIP) to mitochondrial fuel selection and regulation of specific oxidoreductase enzymes in skeletal muscle. *J. Biol. Chem.* **2014**, *289*, 8106–20.

(31) Yao, D.; Gu, Z.; Nakamura, T.; Shi, Z. Q.; Ma, Y.; Gaston, B.; Palmer, L. A.; Rockenstein, E. M.; Zhang, Z.; Masliah, E.; Uehara, T.; Lipton, S. A. Nitrosative stress linked to sporadic Parkinson's disease: S-nitrosylation of parkin regulates its E3 ubiquitin ligase activity. *Proc. Natl. Acad. Sci. U.S.A.* **2004**, *101*, 10810–4.

(32) McDonagh, B.; Martinez-Acedo, P.; Vazquez, J.; Padilla, C. A.; Sheehan, D.; Barcena, J. A. Application of iTRAQ reagents to relatively quantify the reversible redox state of cysteine residues. *Int. J. Proteomics* **2012**, *2012*, 514847.

(33) Lushchak, O. V.; Piroddi, M.; Galli, F.; Lushchak, V. I. Aconitase post-translational modification as a key in linkage between Krebs cycle, iron homeostasis, redox signaling, and metabolism of reactive oxygen species. *Redox Rep.* **2014**, *19*, 8–15.

(34) van der Linde, K.; Gutsche, N.; Leffers, H. M.; Lindermayr, C.; Muller, B.; Holtgrefe, S.; Scheibe, R. Regulation of plant cytosolic aldolase functions by redox-modifications. *Plant Physiol. Biochem.* **2011**, *49*, 946–57.

(35) Marino, S. M.; Gladyshev, V. N. Cysteine function governs its conservation and degeneration and restricts its utilization on protein surfaces. *J. Mol. Biol.* **2010**, *404*, 902–16.

(36) Martinez-Acedo, P.; Nunez, E.; Gomez, F. J.; Moreno, M.; Ramos, E.; Izquierdo-Alvarez, A.; Miro-Casas, E.; Mesa, R.; Rodriguez, P.; Martinez-Ruiz, A.; Dorado, D. G.; Lamas, S.; Vazquez, J. A novel strategy for global analysis of the dynamic thiol redox proteome. *Mol. Cell. Proteomics* **2012**, *11*, 800–13.

(37) Paulsen, C. E.; Carroll, K. S. Cysteine-mediated redox signaling: chemistry, biology, and tools for discovery. *Chem. Rev.* **2013**, *113*, 4633–79.

(38) Leichert, L. I.; Gehrke, F.; Gudiseva, H. V.; Blackwell, T.; Ilbert, M.; Walker, A. K.; Strahler, J. R.; Andrews, P. C.; Jakob, U. Quantifying changes in the thiol redox proteome upon oxidative stress in vivo. *Proc. Natl. Acad. Sci. U.S.A.* **2008**, *105*, 8197–202.

(39) McDonagh, B.; Padilla, C. A.; Pedrajas, J. R.; Barcena, J. A. Biosynthetic and iron metabolism is regulated by thiol proteome changes dependent on glutaredoxin-2 and mitochondrial peroxiredoxin-1 in *Saccharomyces cerevisiae. J. Biol. Chem.* **2011**, *286*, 15565–76.

(40) McDonagh, B.; Ogueta, S.; Lasarte, G.; Padilla, C. A.; Barcena, J. A. Shotgun redox proteomics identifies specifically modified cysteines in key metabolic enzymes under oxidative stress in *Saccharomyces cerevisiae. J. Proteomics* **2009**, *72*, 677–89.

(41) Pan, K. T.; Chen, Y. Y.; Pu, T. H.; Chao, Y. S.; Yang, C. Y.; Bomgarden, R. D.; Rogers, J. C.; Meng, T. C.; Khoo, K. H. Mass spectrometry-based quantitative proteomics for dissecting multiplexed redox cysteine modifications in nitric oxide-protected cardiomyocyte under hypoxia. *Antiox. Redox Signaling* **2014**, *20*, 1365–81.

(42) Sakellariou, G. K.; Vasilaki, A.; Palomero, J.; Kayani, A.; Zibrik, L.; McArdle, A.; Jackson, M. J. Studies of mitochondrial and nonmitochondrial sources implicate nicotinamide adenine dinucleotide phosphate oxidase(s) in the increased skeletal muscle superoxide generation that occurs during contractile activity. *Antiox. Redox Signaling* **2013**, *18*, 603–21.

(43) Morris, B. J. Seven sirtuins for seven deadly diseases of aging. *Free Radical Biol. Med.* **2013**, *56*, 133–71.

(44) Lee, D.; Goldberg, A. L. SIRT1 protein, by blocking the activities of transcription factors FoxO1 and FoxO3, inhibits muscle atrophy and promotes muscle growth. *J. Biol. Chem.* **2013**, *288*, 30515–26.

(45) Shao, D.; Oka, S.; Liu, T.; Zhai, P.; Ago, T.; Sciarretta, S.; Li, H.; Sadoshima, J. A redox-dependent mechanism for regulation of AMPK activation by Thioredoxin1 during energy starvation. *Cell Metab.* **2014**, *19*, 232–45.

(46) Wu, N.; Zheng, B.; Shaywitz, A.; Dagon, Y.; Tower, C.; Bellinger, G.; Shen, C. H.; Wen, J.; Asara, J.; McGraw, T. E.; Kahn, B. B.; Cantley, L. C. AMPK-dependent degradation of TXNIP upon energy stress leads to enhanced glucose uptake via GLUT1. *Mol. Cell* **2013**, *49*, 1167–75.

(47) Winklhofer, K. F. Parkin and mitochondrial quality control: toward assembling the puzzle. *Trends Cell Biol.* **2014**, *24*, 332–341.

(48) Miller-Fleming, L.; Antas, P.; Pais, T. F.; Smalley, J. L.; Giorgini, F.; Outeiro, T. F. Yeast DJ-1 superfamily members are required for diauxic-shift reprogramming and cell survival in stationary phase. *Proc. Natl. Acad. Sci. U.S.A.* **2014**, *111*, 7012–7.

(49) Klamt, F.; Zdanov, S.; Levine, R. L.; Pariser, A.; Zhang, Y.; Zhang, B.; Yu, L. R.; Veenstra, T. D.; Shacter, E. Oxidant-induced apoptosis is mediated by oxidation of the actin-regulatory protein cofilin. *Nat. Cell Biol.* **2009**, *11*, 1241–6.

(50) Vincent, B.; De Bock, K.; Ramaekers, M.; Van den Eede, E.; Van Leemputte, M.; Hespel, P.; Thomis, M. A. ACTN3 (R577X) genotype is associated with fiber type distribution. *Physiol. Genomics* **2007**, *32*, 58–63.

(51) Corcoran, A.; Cotter, T. G. Redox regulation of protein kinases. *FEBS J.* **2013**, *280*, 1944–65.

(52) Watson, J. D. Type 2 diabetes as a redox disease. *Lancet* **2014**, *383*, 841–3.

(53) Terrill, J. R.; Radley-Crabb, H. G.; Iwasaki, T.; Lemckert, F. A.; Arthur, P. G.; Grounds, M. D. Oxidative stress and pathology in muscular dystrophies: focus on protein thiol oxidation and dysferlinopathies. *FEBS J.* **2013**, *280*, 4149–64.

(54) Mates, J. M.; Segura, J. A.; Alonso, F. J.; Marquez, J. Intracellular redox status and oxidative stress: implications for cell proliferation, apoptosis, and carcinogenesis. *Arch. Toxicol.* **2008**, *82*, 273–99.

(55) O'Neill, H. M.; Holloway, G. P.; Steinberg, G. R. AMPK regulation of fatty acid metabolism and mitochondrial biogenesis: implications for obesity. *Mol. Cell. Endocrinol.* **2013**, *366*, 135–51.

(56) Gil-del Valle, L.; de la, C. M. L.; Toledo, A.; Vilaro, N.; Tapanes, R.; Otero, M. A. Altered redox status in patients with diabetes mellitus type I. *Pharmacol. Res.* **2005**, *51*, 375–80.